

# STUDY OF THE PROCESS $e^+e^- \rightarrow \pi^+\pi^-\pi^+\pi^-$ IN THE C.M. ENERGY RANGE 920–1060 MEV WITH THE CMD-3 DETECTOR

R.R.Akhmetshin<sup>a,b</sup>, A.N.Amirkhanov<sup>a,b</sup>, A.V.Anisenkov<sup>a,b</sup>,  
 V.M.Aulchenko<sup>a,b</sup>, V.Sh.Banzarov<sup>a</sup>, N.S.Bashtovoy<sup>a</sup>,  
 D.E.Berkaev<sup>a,b</sup>, A.E.Bondar<sup>a,b</sup>, A.V.Bragin<sup>a</sup>, S.I.Eidelman<sup>a,b</sup>,  
 D.A.Epifanov<sup>a,b</sup>, L.B.Epshteyn<sup>a,b,c</sup>, A.L.Erofeev<sup>a,b</sup>,  
 G.V.Fedotovich<sup>a,b</sup>, S.E.Gayazov<sup>a,b</sup>, A.A.Grebenuk<sup>a,b</sup>,  
 S.S.Gribanov<sup>a,b</sup>, D.N.Grigoriev<sup>a,b,c</sup>, F.V.Ignatov<sup>a,b</sup>, V.L.Ivanov<sup>a,b</sup>,  
 S.V.Karpov<sup>a</sup>, A.S.Kasaev<sup>a</sup>, V.F.Kazanin<sup>a,b</sup>, I.A.Koop<sup>a,b</sup>,  
 O.A.Kovalenko<sup>a,b</sup>, A.A.Korobov<sup>a,b</sup>, A.N.Kozyrev<sup>a,c</sup>,  
 E.A.Kozyrev<sup>a,b</sup>, P.P.Krokovny<sup>a,b</sup>, A.E.Kuzmenko<sup>a,b</sup>,  
 A.S.Kuzmin<sup>a,b</sup>, I.B.Logashenko<sup>a,b</sup>, A.P.Lysenko<sup>a</sup>, P.A.Lukin<sup>a,b</sup>,  
 K.Yu.Mikhailov<sup>a</sup>, V.S.Okhapkin<sup>a</sup>, Yu.N.Pestov<sup>a</sup>,  
 E.A.Perevedentsev<sup>a,b</sup>, A.S.Popov<sup>a,b</sup>, G.P.Razuvayev<sup>a,b</sup>,  
 Yu.A.Rogovsky<sup>a</sup>, A.A.Ruban<sup>a</sup>, N.M.Ryskulov<sup>a</sup>,  
 A.E.Ryzhenenkov<sup>a,b</sup>, V.E.Shebalin<sup>a,b</sup>, D.N.Shemyakin<sup>a,b</sup>,  
 B.A.Shwartz<sup>a,b</sup>, D.B.Shwartz<sup>a,b</sup>, A.L.Sibidanov<sup>a,d</sup>,  
 Yu.M.Shatunov<sup>a</sup>, E.P.Solodov<sup>a,b,1</sup>, V.M.Titov<sup>a</sup>, A.A.Talyshev<sup>a,b</sup>,  
 A.I.Vorobiov<sup>a</sup>, Yu.V.Yudin<sup>a,b</sup>

<sup>a</sup>*Budker Institute of Nuclear Physics, SB RAS, Novosibirsk, 630090, Russia*

<sup>b</sup>*Novosibirsk State University, Novosibirsk, 630090, Russia*

<sup>c</sup>*Novosibirsk State Technical University, Novosibirsk, 630092, Russia*

<sup>d</sup>*University of Victoria, Victoria, BC, Canada V8W 3P6*

---

## Abstract

A cross section of the process  $e^+e^- \rightarrow \pi^+\pi^-\pi^+\pi^-$  has been measured using  $6798 \pm 93$  signal events from a data sample corresponding to an integrated luminosity of  $9.8 \text{ pb}^{-1}$  collected with the CMD-3 detector in the center-of-

---

<sup>1</sup>Corresponding author: solodov@inp.nsk.su

mass energy range 920–1060 MeV. The measured cross section exhibits an interference pattern of the  $\phi(1020) \rightarrow \pi^+\pi^-\pi^+\pi^-$  decay with a non-resonant process  $e^+e^- \rightarrow \pi^+\pi^-\pi^+\pi^-$ , from which we obtain the branching fraction of the doubly suppressed decays (by G-parity and OZI rule):

$$\mathcal{B}(\phi \rightarrow \pi^+\pi^-\pi^+\pi^-) = (6.5 \pm 2.7 \pm 1.6) \times 10^{-6}.$$


---

## 1. Introduction

Production of four charged pions in  $e^+e^-$  annihilation has been studied with good statistics with the CMD-2 [1] and SND detectors [2] as well as using initial-state radiation (ISR) with BaBar [3] at which a low (about 3%) systematic uncertainty was achieved on the  $e^+e^- \rightarrow \pi^+\pi^-\pi^+\pi^-$  cross section in the wide center-of-mass energy (E<sub>c.m.</sub>) range. Earlier experiments are discussed in Ref. [4].

However, a detailed study of this cross section in the vicinity of the  $\phi(1020)$  resonance peak was performed by the CMD-2 detector only (E<sub>c.m.</sub> = 984–1060 MeV) [5], and  $\mathcal{B}(\phi \rightarrow \pi^+\pi^-\pi^+\pi^-) = (4.0^{+2.8}_{-2.2}) \times 10^{-6}$  has been obtained. The  $\phi(1020)$  decay to four charged pions is doubly suppressed by G-parity and the OZI-rule, and new measurements are interesting.

In this paper we report an analysis of the data sample of 9.8 pb<sup>-1</sup> collected at the CMD-3 detector in the E<sub>c.m.</sub> = 920–1060 MeV energy range. The data were collected in the energy scan of 22 c.m. energy points performed at the VEPP-2000 collider [7] and used for a precision study of the process  $e^+e^- \rightarrow \phi \rightarrow K_S^0 K_L^0$  [8] and obtaining the world best upper limit for the  $e^+e^- \rightarrow \eta'(958)$  process [9].

The general-purpose detector CMD-3 has been described in detail elsewhere [10]. Its tracking system consists of a cylindrical drift chamber (DC) [11] and double-layer multiwire proportional Z-chamber, both also used for a trigger, and both inside a thin (0.2 X<sub>0</sub>) superconducting solenoid with a field of 1.3 T. The electromagnetic calorimeter (EMC) includes three systems. The liquid xenon (LXe) barrel calorimeter with a thickness of 5.4 X<sub>0</sub> has a fine electrode structure, providing 1–2 mm spatial resolution [12], and shares the cryostat vacuum volume with the superconducting solenoid. The barrel

CsI crystal calorimeter with a thickness of  $8.1 X_0$  is placed outside the LXe calorimeter, and the endcap BGO calorimeter with a thickness of  $13.4 X_0$  is installed inside the solenoid [13]. The luminosity is measured using events of Bhabha scattering at large angles [14] with about 1% accuracy. The c.m. energy has been monitored by using the Back-Scattering-Laser-Light system [15] with about 0.06 MeV systematic uncertainty. To obtain a detection efficiency, we have developed Monte Carlo (MC) simulation of our detector based on the GEANT4 [16] package, in which the interaction of generated particles with the detector and its response are implemented. MC simulation includes soft-photon radiation by the electron or positron, calculated according to Ref. [17].

## 2. Selection of $e^+e^- \rightarrow \pi^+\pi^-\pi^+\pi^-$ events

Candidates for the process under study are required to have three or four tracks of charged particles in the DC with the following requirements: the ionization losses of each track in the DC to be consistent with the pion hypothesis; a track momentum is larger than 40 MeV/c; a minimum distance from a track to the beam axis in the transverse plane is less than 0.25 cm; and a minimum distance from a track to the center of the interaction region along the beam axis Z is less than 12 cm. Reconstructed momenta and angles of the tracks for three- and four-track candidates are used for further selection.

A background in the studied energy region comes from the processes  $e^+e^- \rightarrow \pi^+\pi^-\pi^0$ ,  $e^+e^- \rightarrow K_S^0 K_L^0$ , and  $e^+e^- \rightarrow K^+K^-$  with extra tracks from decays or nuclear interaction of pions or kaons, as well as from a conversion of the photons from  $\pi^0$ -decay in the detector material. Charged kaons are efficiently suppressed by the ionization losses in the DC. To suppress neutral kaons, we remove events with invariant mass of any two pion candidates within 20 MeV from the  $K^0$  mass and having total momentum inside the 20 MeV/c window of the expected kaon momentum for the  $e^+e^- \rightarrow K_S^0 K_L^0$  reaction. To reduce the background from the reaction  $e^+e^- \rightarrow \pi^+\pi^-\pi^0$ , we require a missing mass for any two pion candidates to be greater than two

pion masses. After this requirement the remaining contribution from three pions is less than 0.3% to number of four-track candidates.

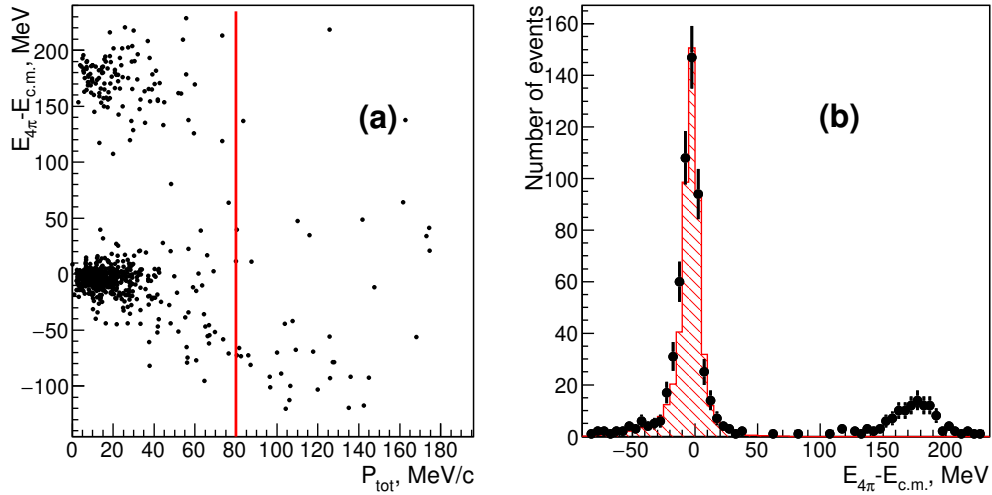


Figure 1: (a) Scatter plot of the difference between the total energy and c.m. energy ( $E_{4\pi} - E_{c.m.}$ ) versus total momentum for four-track events. The line shows the boundary of the applied selection; (b) Projection plot of (a) after selection. The histogram shows the MC-simulated distribution normalized to data.

For four- or three-track candidates we calculate the total energy and total momentum assuming all tracks to be pions:

$$E_{3,4\pi} = \sum_{i=1}^{3,4} \sqrt{p_i^2 + m_\pi^2}, \quad P_{\text{tot}} = \left| \sum_{i=1}^{3,4} \vec{p}_i \right|.$$

Figure 1(a) shows a scatter plot of the difference between the total energy and c.m. energy  $E_{4\pi} - E_{c.m.}$  versus total momentum for four-track candidates for  $E_{c.m.} = 958$  MeV. A clear signal of four-pion events is seen as a cluster of dots near zero. Events with a radiative photon have non-zero total momentum and total energy, which is always smaller than the nominal one. A momentum of any pion incorrectly reconstructed due to the interaction with the detector material or DC resolution leads to momentum-energy correlated “tails” in both directions.

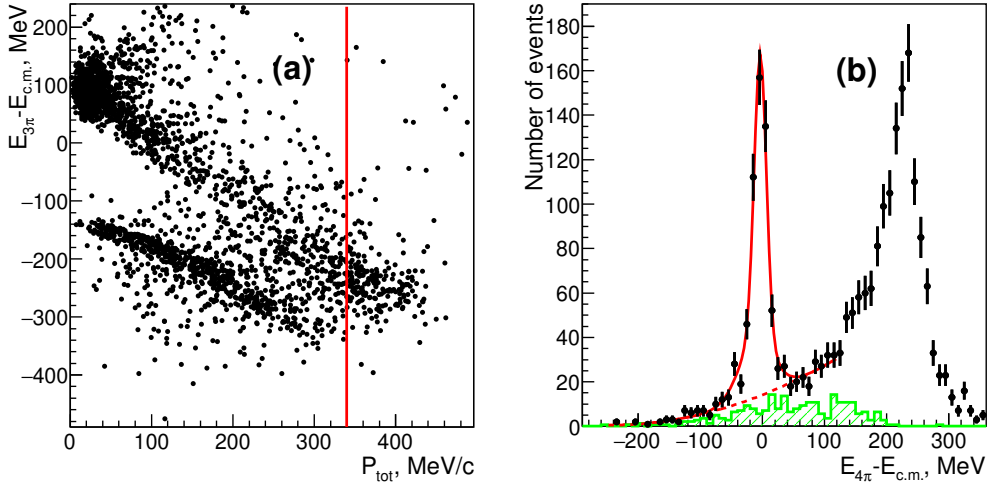


Figure 2: (a) Scatter plot of the difference of the total energy and c.m. energy ( $E_{3\pi} - E_{c.m.}$ ) versus total momentum for three-track events; (b) Difference between the total energy of three tracks plus missing track energy and c.m. energy ( $E_{4\pi} - E_{c.m.}$ ) (points). The line shows a fit function used to obtain the number of signal events. The shaded histogram shows an estimate of background events from the  $e^+e^- \rightarrow 3\pi$  process.

A cluster of dots is also observed shifted up from the four-pion signal. These events are from the process  $e^+e^- \rightarrow e^+e^-e^+e^-$  where electrons and positrons are produced due to two-photon processes as well as a conversion of radiative photons from the  $e^+e^- \rightarrow e^+e^-\gamma$  reaction on the detector material, and a conversion of photons from the process  $e^+e^- \rightarrow \gamma\gamma$ . Not all of these tracks can be identified as electron or positron in the EMC, but kinematically these events are well separated from the signal events, therefore we do not apply additional requirements.

We select events with total momentum less than 80 MeV/c and show the difference  $E_{4\pi} - E_{c.m.}$  in Fig. 1(b). The experimental points are in good agreement with the corresponding Monte Carlo simulated distribution shown by the histogram. We require  $-100 < E_{4\pi} - E_{c.m.} < 50$  MeV to determine the number of four-pion events,  $N_{4\pi}$ . Four-track events have practically no background: we estimate it from MC simulation of the major background

process  $e^+e^- \rightarrow \pi^+\pi^-\pi^0$  (a photon from the  $\pi^0$  decay converts to an  $e^+e^-$  pair at the beam pipe), and find a contribution of less than 0.3% at the peak of the  $\phi$  resonance. We use this value as an estimate of the corresponding systematic uncertainty.

To determine the number of four-pion events with one missing track, a sample with three selected tracks is used. A track can be lost if it flies at small polar angles outside the efficient DC region, decays in flight, due to incorrect reconstruction, nuclear interactions or by overlapping with another track. Four-pion candidates in the three-track sample have energy deficit correlated with the total (missing) momentum of three detected pions. Figure 2(a) shows a scatter plot of the difference  $E_{3\pi} - E_{\text{c.m.}}$  between the total energy and c.m. energy versus total momentum for three-track events. A band of signal events is clearly seen. This sample has a large contribution from the processes with electrons and positrons mentioned above as well as from the conversion of photons from the  $\pi^0$  decays. We apply an additional requirement on the maximum value of the total momentum of three tracks, assuming a four-pion final state. This requirement is shown by a line in Fig. 2(a).

Using total momentum of four-track candidates, we calculate the energy of a missing pion, and add it to the energy of three detected pions: the difference of obtained energy and c.m. energy is shown in Fig. 2(b) by points. The expected background contribution from three pions is shown by the shaded histogram in Fig. 2(b).

To obtain the number of four-pion events from the three-track sample, we fit the distribution shown in Fig. 2(b) with a sum of the functions describing a signal peak and background. The signal line shape is taken from the MC simulation of the four-pion process, and is well described by a sum of two Gaussian distributions. The photon emission by initial electrons and positrons is taken into account in the MC simulation, and gives a small asymmetry observed in the distributions of Fig. 1(b) and Fig. 2(b). All parameters of the signal function are fixed except for the number of events and the resolution of the narrowest Gaussian. A second-order polynomial is used to describe the background distribution.

Variation of the polynomial fit parameters for the experimental and MC-simulated background distributions, removing or applying background suppressing requirements lead to about 3% uncertainty on the number of signal events.

We find  $3690 \pm 61$  four-track events and  $3108 \pm 69$  three-track events corresponding to the process  $e^+e^- \rightarrow \pi^+\pi^-\pi^+\pi^-$  in the  $E_{\text{c.m.}} = 920\text{--}1060$  MeV energy range.

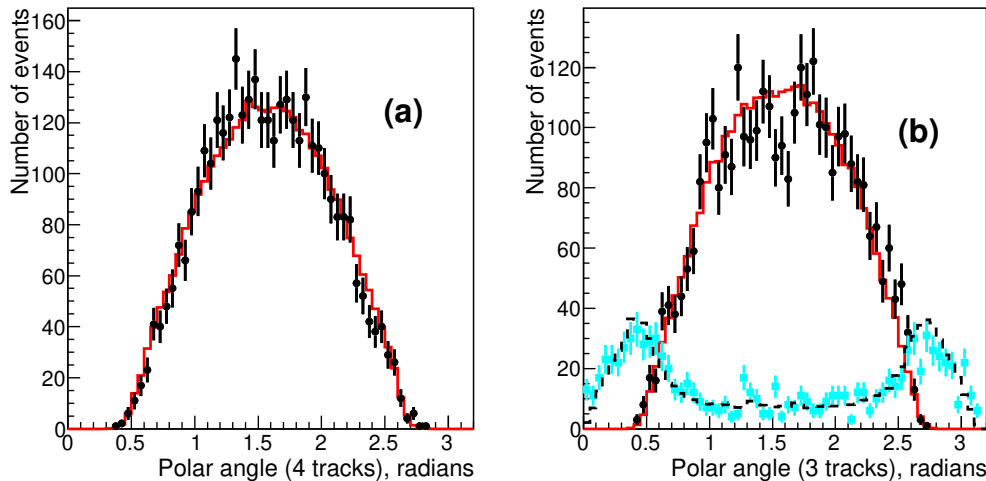


Figure 3: (a) Polar angle distribution for four-pion events with four detected tracks for data (points) and MC simulation (histogram); (b) Polar angle distribution for four-pion events with three detected tracks for data (circles) and MC simulation (solid histogram). The polar angle distribution for a missing track is shown by squares (data) and the dashed histogram (MC simulation).

### 3. Detection efficiency

In our experiment, the acceptance of the DC for the charged tracks is not 100%, and the detection efficiency depends on the dynamics of four-pion production. The dynamics of the process  $e^+e^- \rightarrow \pi^+\pi^-\pi^+\pi^-$  are relatively well studied in previous experiments [4, 3], and the  $a_1(1260)^\pm\pi^\mp$  final state

has been shown to dominate. Our energy range is well below the nominal threshold of this reaction, and with our data sample we cannot observe any difference in any distribution for other final states, like  $\rho(770)f_0(600)$  or phase-space production of four pions.

Figure 3(a) presents the polar angle ( $\theta_\pi$ ) distribution for four-pion events with all detected tracks. The result of the MC simulation in the model with the  $a_1(1260)\pi$  final state, presented by the histogram well describes the observed distribution. Figure 3(b) presents the polar angle distribution for three detected tracks (circles for data, the solid histogram for the MC simulation) after background subtraction. The polar angle distribution for the missing track is shown by squares (data) and the dashed histogram (MC). With our DC acceptance we have about the same number of four-pion events with one missing track compared to events with all tracks detected.

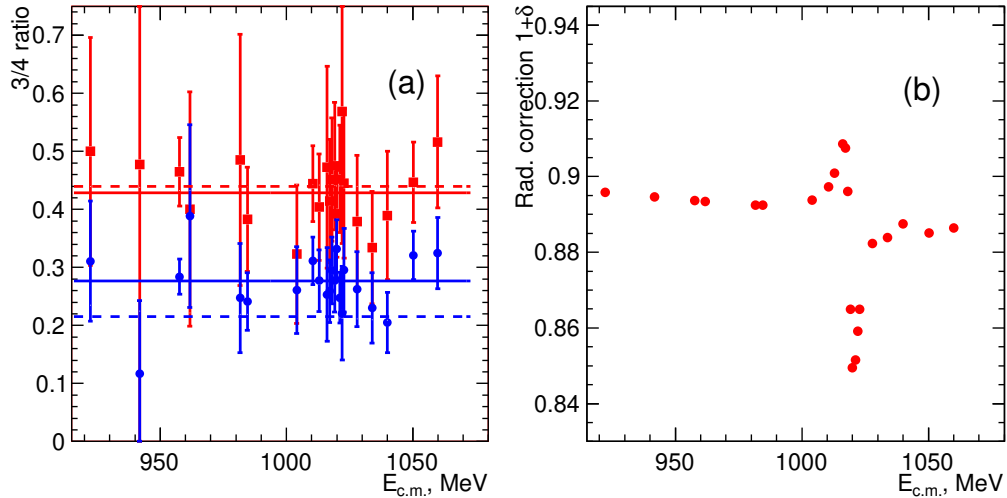


Figure 4: (a) Ratio of numbers of three- to four-detected-track events for data (points with errors) and MC simulation (the dashed line at 0.215) when all tracks are within the DC acceptance. The ratio of number of the events with one track outside the DC acceptance to number of the events with all tracks inside the DC acceptance (squares) and the corresponding MC-simulation value (the dashed line at 0.441). (b) Radiative correction  $1 + \delta$  for the experimental energy points.

Figure 4(a) shows a ratio of the number of three-track events,  $N_{3\text{trDC}}$ , with a missing track inside a DC acceptance ( $0.7 < \theta_\pi < 2.44$  radians) to the number of four-track events,  $N_{4\text{tr}}$ , for data (circles) and MC-simulation (a dashed line at 0.215). This ratio for data exhibits very small variation with energy, but the average value of  $0.274 \pm 0.012$  differs from that for the MC-simulation. Based on these numbers we conclude that our MC-simulation overestimates a track reconstruction efficiency: 0.951 vs  $0.936 \pm 0.004$  in data. This difference does not depend on the primary generator model. We add events with a missing track inside the DC acceptance volume to a four-track sample, and this sum,  $N_{4\text{tr}} + N_{3\text{trDC}}$ , corresponds to about 98% of events with all four pions inside the DC acceptance: a probability to detect only one or two tracks from four is very low. A correction for the data-MC difference,  $\epsilon_{1\text{corr}}$ , is about 1%, and we assign a 1% systematic uncertainty to this value.

The number of remaining events with a missing track outside the DC acceptance,  $N_{3\text{tr}}$ , can be sensitive to the production dynamics and is used to validate MC-simulated efficiency. Figure 4(a) shows a ratio of the number of three-track events with a missing track outside the DC acceptance to the sum of the numbers of four- and three-track events inside the DC acceptance for data (squares) and MC-simulation (the dashed line at 0.441). This ratio is also stable vs  $E_{\text{c.m.}}$ , and the average value of  $0.429 \pm 0.022$  is in agreement with that obtained from the MC-simulation. The experimental value is also in agreement with the MC-simulation for the  $\rho(770)f_0(600)$  final state (0.447) and with the phase-space model (0.435). Assuming single track reconstruction efficiency shown above, the data-MC correction for these three detected tracks,  $\epsilon_{2\text{corr}}$ , is about  $(5 \pm 3)\%$ ; the error is taken as a systematic uncertainty on this correction.

We use the model with an  $a_1(1260)\pi$  final state, and calculate the detection efficiency from the MC-simulated events as a ratio of all three- and four-track events to the total number of generated events. Note that if a sum of four- and three-track events is taken for the calculation, the efficiency increases to  $\epsilon = 77.3\%$ , independently of the c.m. energy, and the data-MC inconsistencies in the DC reconstruction efficiency and in the model-dependent

angular distributions are significantly reduced.

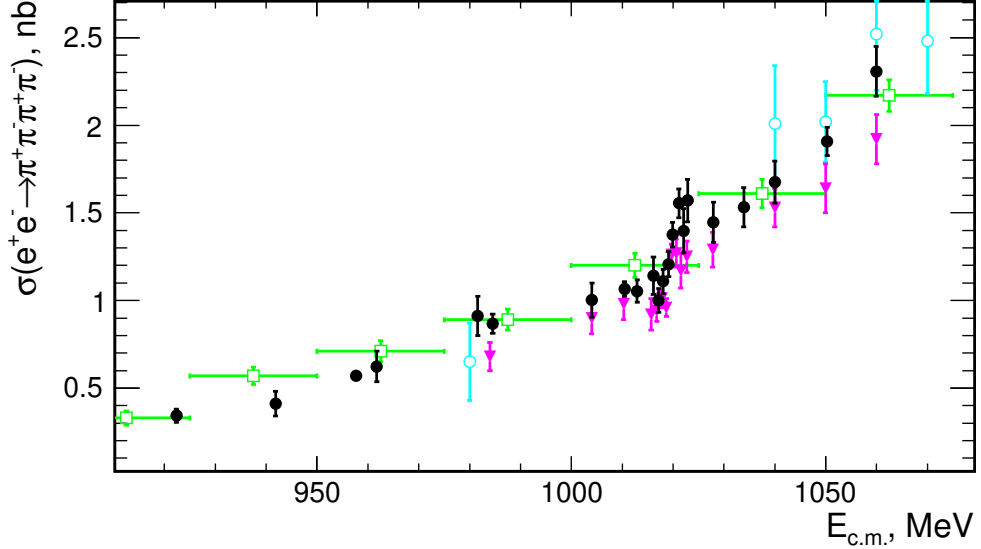


Figure 5: The  $e^+e^- \rightarrow \pi^+\pi^-\pi^+\pi^-$  cross section measured with the CMD-3 detector at VEPP-2000 (dots). The results of the BaBar measurement [3] are shown by open squares, measurements by CMD-2 are shown by triangles [5] and by open circles [1].

#### 4. Cross Section Calculation

At each  $E_{\text{c.m.}}$  energy the cross section is calculated using four- and three-track events as

$$\sigma = \frac{(N_{4\text{tr}} + N_{3\text{trDC}})/(1 - \epsilon_{1\text{corr}}) + N_{3\text{tr}}/(1 - \epsilon_{2\text{corr}})}{L \cdot \epsilon \cdot (1 + \delta)},$$

where  $(1 - \epsilon_{1\text{corr}})$  is the data-MC correction to the number of events with four pions inside the DC acceptance,  $(1 - \epsilon_{2\text{corr}})$  is the data-MC correction to the number of events with one pion out of the DC acceptance,  $L$  is the integrated luminosity at this energy,  $\epsilon$  is the detection efficiency, and  $(1 + \delta)$  is the radiative correction calculated according to [17] and shown in Fig. 4 (b). The energy dependence of the radiative correction reflects an interference

pattern in the cross section. To calculate the correction, we use CMD-2 data [5] as a first approximation and then use our cross section data for the following iterations.

Our result is shown in Fig. 5 by solid circles in comparison with the previous measurements. The c.m. energy, integrated luminosity, number of four- and three-track events, radiative correction and obtained cross section for each energy are listed in Table 1.

The obtained cross section is in overall agreement with the results of the high-precision measurement performed by the BaBar Collaboration [3], shown in Fig. 5 by open squares, and reanalyzed data of CMD-2 [1] (open circles). Our cross section is about 10% higher than the CMD-2 measurement in the  $\phi$ -resonance region [5] (triangles), because these data were not reanalyzed, and the tracking efficiency was somehow overestimated.

## 5. Systematic errors

The following sources of systematic uncertainties are considered.

- Using three- and four-track events for the cross section calculation has reduced the overall model dependence uncertainty to about 1%: the  $a_1(1260)\pi$ ,  $\rho(770)f_0(600)$  and phase-space models are tested.
- Using responses of two independent triggers (neutral and charged) for our event sample, we found trigger efficiency close to unity with a negligible contribution to the systematic error.
- The overall uncertainty on the determination of the integrated luminosity comes from the selection criteria of Bhabha events, radiative corrections and calibrations of DC and calorimeters, and does not exceed 1% [14].
- The admixture of the background events not subtracted from the four-track sample is estimated as a 0.3% systematic uncertainty on the number of four-track events, with additional 1% uncertainty from the data-MC efficiency correction.

- The uncertainty on the background subtraction for three-track events is studied by the variation of functions used for a background description in Fig. 2(b) and is estimated as 3% of the number of three-track events. An additional 3% uncertainty comes from the data-MC efficiency correction.
- A radiative correction uncertainty is estimated as about 1%.

The above systematic uncertainties summed in quadrature and weighted with the number of three- and four-track events give an overall systematic error of about 3.6%.

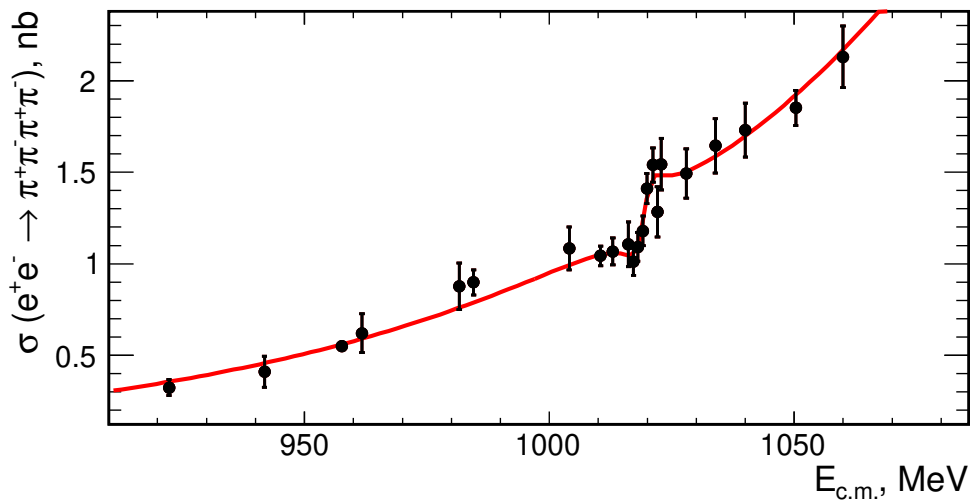


Figure 6: The  $e^+e^- \rightarrow \pi^+\pi^-\pi^+\pi^-$  cross section measured with the CMD-3 detector at VEPP-2000 (dots) with the fit function described in the text.

## 6. Fit to $\phi \rightarrow \pi^+\pi^-\pi^+\pi^-$ decay rate

The obtained cross section exhibits a clear interference pattern of the  $\phi(1020) \rightarrow \pi^+\pi^-\pi^+\pi^-$  transition with the non-resonant cross section. We fit

the experimental cross section with the function

$$\sigma(E_{c.m.}) = \sigma_0 \cdot f(E_{c.m.}) \cdot \left| 1 - Z \cdot \frac{m_\phi \Gamma_\phi}{m_\phi^2 - E_{c.m.}^2 - iE_{c.m.} \Gamma_\phi} \right|^2,$$

where  $\sigma_0$  is a non-resonant cross section at the  $\phi$  resonance mass  $E_{c.m.} = m_\phi = 1019.456$  MeV/c<sup>2</sup> with  $\Gamma_\phi = 4.24$  MeV width [6],  $f(E_{c.m.}) = e^{A(E_{c.m.} - m_\phi)}$ ,  $A$  is a slope parameter, describes the energy dependence of the non-resonant cross section, and  $Z$  is a complex amplitude of the  $\phi(1020) \rightarrow \pi^+\pi^-\pi^+\pi^-$  transition. The fit yields

$$\sigma_0 = 1.263 \pm 0.027 \text{ nb},$$

$$\text{Re } Z = 0.146 \pm 0.030,$$

$$\text{Im } Z = -0.002 \pm 0.024.$$

The second solution gives the unphysical values for  $Z$  and is ignored. The  $\phi \rightarrow \pi^+\pi^-\pi^+\pi^-$  decay rate is calculated as

$$\mathcal{B}(\phi \rightarrow \pi^+\pi^-\pi^+\pi^-) = \sigma_0 \cdot |Z|^2 / \sigma_\phi = (6.5 \pm 2.7 \pm 1.6) \times 10^{-6},$$

where  $\sigma_\phi = 12\pi \mathcal{B}(\phi \rightarrow e^+e^-) / m_\phi^2 = 4172 \pm 42$  nb is a peak cross section of  $\phi(1020)$ . The first error is statistical, while the second error is our estimate of the systematic uncertainty, based on the uncertainty on the cross section discussed in Sec. 5. The  $E_{c.m.}$  energy spread (about 300 keV) contributes less than 4% to the observed  $\phi$  signal, and is negligibly small compared to other uncertainties. Figure 6 shows our experimental points with the fit curve. The result is in overall agreement with the previous measurement  $\mathcal{B}(\phi \rightarrow \pi^+\pi^-\pi^+\pi^-) = (4.0^{+2.8}_{-2.2}) \times 10^{-6}$  [5], and does not contradict to the value, assuming a single-photon reaction:  $\mathcal{B}(\phi \rightarrow \gamma^* \rightarrow 4\pi) = 9 \cdot \mathcal{B}(\phi \rightarrow e^+e^-)^2 / \alpha^2 \cdot \sigma_0 / \sigma_\phi = 4.8 \times 10^{-6}$ , which assumes  $\text{Im } Z=0$ .

## Conclusion

The total cross section of the process  $e^+e^- \rightarrow \pi^+\pi^-\pi^+\pi^-$  has been measured using a data sample corresponding to an integrated luminosity of 9.8 pb<sup>-1</sup> collected by the CMD-3 detector at the VEPP-2000  $e^+e^-$  collider in the 920–1060 MeV c.m. energy range. The three- and four-track events are used to estimate the model-dependent and other uncertainties on the

cross section calculation, giving a 3.6% overall systematic uncertainty. The measured cross section is in overall agreement with previous experiments in the energy range studied, exhibits the interference pattern of the  $\phi(1020) \rightarrow \pi^+\pi^-\pi^+\pi^-$  transition with the non-resonant cross section, and a new value  $\mathcal{B}(\phi \rightarrow \pi^+\pi^-\pi^+\pi^-) = (6.5 \pm 2.7 \pm 1.6) \times 10^{-6}$  has been obtained.

#### *Acknowledgments*

We thank the VEPP-2000 personnel for the excellent machine operation. Part of this work is supported by the Russian Foundation for Basic Research grants RFBR 15-02-05674-a and RFBR 16-02-00160-a.

## REFERENCES

- [1] R. R. Akhmetshin *et al.* (CMD-2 Collaboration), Phys. Lett. B**595**, 101 (2004).
- [2] M. N. Achasov *et al.* (SND Collaboration), JETP **96**, 789 (2003).
- [3] B. Aubert *et al.* (BaBar Collaboration), Phys. Rev. D**85**, 112009 (2012).
- [4] R. R. Akhmetshin *et al.* (CMD-2 Collaboration), Phys. Lett. B**475**, 190 (2000).
- [5] R. R. Akhmetshin *et al.* (CMD-2 Collaboration), Phys. Lett. B**491**, 81 (2000).
- [6] C. Patrignani *et al.* (Particle Data Group), Chin. Phys. C**40**, 100001 (2016).
- [7] V.V. Danilov *et al.*, Proceedings EPAC96, Barcelona, p.1593 (1996); I.A.Koop, Nucl. Phys. B (Proc. Suppl.) **181-182**, 371 (2008).
- [8] E. A. Kozyrev *et al.* (CMD-2 Collaboration), Phys. Lett. B**760**, 314 (2016).
- [9] R. R. Akhmetshin *et al.* (CMD-2 Collaboration), Phys. Lett. B**740**, 273 (2015).
- [10] B. I. Khazin, Nucl. Phys. B (Proc. Suppl.) **181-182**, 376 (2008).
- [11] F. Grancagnolo *et al.*, Nucl. Instr. Meth. A**623**, 114 (2010).
- [12] A. V. Anisyonkov *et al.*, Nucl. Instr. Meth. A**598**, 266 (2009).

- [13] D. Epifanov (CMD-3 Collaboration), J. Phys. Conf. Ser. **293**, 012009 (2011); V. M. Aulchenko *et al.*, JINST **10**, P10006 (2015); V. E. Shebalin *et al.*, JINST **9**, C10013 (2014).
- [14] R. R. Akhmetshin *et al.*, Nucl. Phys. B (Proc. Suppl.) **225-227**, 69 (2012); G. V. Fedotovich *et al.*, Phys. At. Nucl. **78**, 591 (2015).
- [15] V. Abakumova *et al.*, Phys. Rev. Lett. **110**, 140402 (2013).
- [16] S. Agostinelli *et al.* (GEANT4 Collaboration), Nucl. Instr. Meth. **A506**, 250 (2003).
- [17] E. A. Kuraev and V. S. Fadin, Sov. J. Nucl. Phys. **41**, 466 (1985); S. Actis *et al.*, Eur. Phys. J. **C66**, 585 (2010).

Table 1: The c.m. energy, integrated luminosity, number of four- and three-track events, radiative correction, and  $e^+e^- \rightarrow \pi^+\pi^-\pi^+\pi^-$  cross section, measured with the CMD-3 detector. Only statistical errors are shown.

$E_{\text{c.m.}}, \text{MeV}$	$L, \text{nb}^{-1}$	$N_{4\pi}$	$N_{3\pi} + N_{3\pi DC}$	$(1 + \delta)$	$\sigma, \text{nb}$
922.35	414.1	49	$47.0 \pm 8.0$	0.895	$0.34 \pm 0.04$
941.83	163.1	29	$18.9 \pm 5.5$	0.893	$0.41 \pm 0.07$
957.68	2621	541	$476.3 \pm 26.3$	0.892	$0.57 \pm 0.02$
961.75	128.1	27	$25.5 \pm 5.9$	0.892	$0.62 \pm 0.09$
981.61	115.8	39	$33.2 \pm 6.4$	0.891	$0.91 \pm 0.11$
984.54	468.1	162	$116.3 \pm 11.5$	0.891	$0.87 \pm 0.05$
1004.07	195.4	80	$53.3 \pm 9.3$	0.892	$1.00 \pm 0.10$
1010.47	936.1	352	$314.6 \pm 18.7$	0.895	$1.07 \pm 0.04$
1012.96	485.4	194	$153.5 \pm 15.5$	0.898	$1.05 \pm 0.06$
1016.15	192.1	82	$69.2 \pm 10.7$	0.907	$1.14 \pm 0.11$
1017.16	479.0	185	$144.7 \pm 17.3$	0.909	$1.00 \pm 0.07$
1018.05	478.3	191	$167.8 \pm 17.7$	0.903	$1.11 \pm 0.07$
1019.12	477.9	202	$178.4 \pm 18.1$	0.876	$1.21 \pm 0.07$
1019.90	570.2	269	$229.7 \pm 20.4$	0.858	$1.38 \pm 0.07$
1021.16	475.4	265	$215.3 \pm 19.0$	0.856	$1.55 \pm 0.08$
1022.08	201.6	97	$88.8 \pm 13.3$	0.861	$1.40 \pm 0.13$
1022.85	195.3	106	$92.4 \pm 11.8$	0.865	$1.57 \pm 0.12$
1027.96	195.8	108	$80.0 \pm 11.0$	0.880	$1.44 \pm 0.11$
1033.91	175.5	110	$70.6 \pm 8.2$	0.882	$1.53 \pm 0.11$
1040.03	195.9	133	$89.5 \pm 10.3$	0.885	$1.68 \pm 0.12$
1050.31	499.6	323	$294.5 \pm 20.1$	0.883	$1.91 \pm 0.08$
1059.95	198.9	147	$148.6 \pm 13.9$	0.885	$2.31 \pm 0.14$